

## Improved cytotoxic and optical characteristics of silver-doped TiO<sub>2</sub> nanoparticles on human liver cancer cells

N. Ur-Rehman <sup>a</sup>, A. D. Khalid <sup>b,\*</sup>, M. Sharif <sup>c</sup>, F. Hadi <sup>d</sup>, F. Abid <sup>e</sup>, M. Zahra <sup>f</sup>, Z. Fatima <sup>b</sup>, I. Ahmad <sup>g</sup>, Khalid M. Elhindi <sup>h</sup>

<sup>a</sup> *Institute of Physics, The Islamia university of Bahawalpur Pakistan*

<sup>b</sup> *University Institute of Radiological Sciences and Medical Imaging Technology, The University of Lahore, Lahore Pakistan*

<sup>c</sup> *Department of DNA and Serology Punjab Forensic Science Agency, Lahore Pakistan*

<sup>d</sup> *Faculty of Medicine and Allied health Sciences, The Islamia university of Bahawalpur Pakistan*

<sup>e</sup> *Department of Pharmacy, University of South Asia, Lahore, Pakistan*

<sup>f</sup> *School of pharmacy and medical sciences, Griffith university Australia*

<sup>g</sup> *Department of Physics and Astronomy, Texas Tech University, Lubbock, TX 79409, USA*

<sup>h</sup> *Department of Plant Production, College of Food & Agricultural Sciences, King Saud University, P.O. Box 2460, Riyadh 11451, Saudi Arabia*

The unique properties of nano-sized metal oxide particles differ from those of their bulk counterparts, and they have numerous biomedical applications, particularly in innovative cancer treatments involving Reactive Oxygen Species (ROS) production. This study utilized Ag-doped TiO<sub>2</sub> nanoparticles (NPs), with Ag concentrations ranging from 5% to 20%, to assess their cytotoxicity on human liver cancer cells (HepG2). Characterization results revealed that the doping of Ag did not alter the brookite and rutile phases of TiO<sub>2</sub> NPs, although the band gap decreased as the doping concentration increased. In addition, the cytotoxic activity was improved with high doping levels which are owing to enhanced optical factor. The findings recommend that Ag-doped TiO<sub>2</sub> NPs encourage cytotoxic effect on HepG2 cells.

(Received December 19, 2024; Accepted March 24, 2025)

*Keywords:* TiO<sub>2</sub>, Doping, Band gap, ROS generation, MTT assay

### 1. Introduction

Nanotechnology is an emerging and rapidly advancing field with significant value due to its broad range of applications across different sectors, including industry, food and medicine. Amongst these applications, biomedical are particularly interest to researchers worldwide [1]. Titanium dioxide Nanoparticles (TiO<sub>2</sub> NPs) are famous biomedical agent, specially renowned for their potential of drug delivery and anti-cancer activities [2,3]. Titanium dioxide nanoparticles are biocompatible as well as bio degradable [4]. It is expected that the annual production of TiO<sub>2</sub> NPs will achieve 2.5 million tons in 2025, motivated by increasing market demands [5]. The mainly common crystalline forms of TiO<sub>2</sub> NPs are anatase and rutile. Study shows that anatase TiO<sub>2</sub> NPs are extra biological active and biocompatible as compared to rutile form [6, 7]. The research in photo catalytic applications of TiO<sub>2</sub> NPs is vital due to their applications in solar energy and photodynamic therapy [8, 9]. When photons are exposed, the movement of excited electrons creates holes, which generates reactive oxygen species (ROS) [10, 11]. These generated ROS have potential to cure various diseases by photodynamic therapy, including cancers of liver, cervix and lungs [12, 13]. Researchers are presently focusing to enhance the photo catalytic activity of TiO<sub>2</sub> NPs in biomedical uses, aim to increase ROS generation by doping of metallic and non metallic

---

\* Corresponding author: ad\_khalid82@hotmail.com

<https://doi.org/10.15251/DJNB.2025.201.327>

elements [14, 15]. One main face with TiO<sub>2</sub> NPs is their large band gap, which requires ultraviolet (UV) light for activation [16]. This matter can be tackled by doping TiO<sub>2</sub> NPs, which reduces the band gap and enhances the light response, mainly in visible spectrum [17]. For instance, doping TiO<sub>2</sub> NPs with metals like silver (Ag), platinum (Pt), and gold (Au) improves their spectral response in the visible range [18]. Ag-doped TiO<sub>2</sub> NPs, in particular, have shown antimicrobial properties under visible light [19,20]. Our study extends this by exploring the use of Ag-doped TiO<sub>2</sub> NPs as an anticancer agent. We investigated their cytotoxicity on human liver cancer cells, as cancer is a rapidly spreading and life-threatening disease [21,22]. Several studies have reported similar findings: Bader et al. studied the cytotoxicity of tantalum-doped TiO<sub>2</sub> NPs on human neuroblastoma cells, noting increased cytotoxicity with higher doping levels [23]. Mahjoubian et al. compared pure TiO<sub>2</sub> NPs with tin-doped TiO<sub>2</sub> NPs in zebrafish, finding enhanced cytotoxicity with Sn-doped TiO<sub>2</sub> NPs [24]. Muneer et al. created zinc-doped TiO<sub>2</sub> NPs and observed improved anticancer activity in human liver cancer cells (HepG2) [25]. Batool et al. synthesized Zn-doped TiO<sub>2</sub> NPs via a green method and found stronger antifungal activity compared to un-doped TiO<sub>2</sub> NPs [26]. Shabaninia et al. synthesized Ag-doped TiO<sub>2</sub> NPs apply the sol-gel technique and demonstrated their anticancer properties against L929 cancer cells [27]. This study focuses on TiO<sub>2</sub> NPs doped with Ag at varying concentrations (5% to 20%) and their cytotoxic effects on human liver cancer cells.

## **2. Materials and method**

The titanium dioxide nanoparticles were synthesized using the widely used sol-gel technique. Titanium isopropoxide (C<sub>12</sub>H<sub>28</sub>O<sub>4</sub>Ti), nitric acid (HNO<sub>3</sub>), and ethanol were used as precursors. To begin, 20 ml each of titanium isopropoxide and ethanol were mixed and stirred with 24 ml of distilled water. Then, 10 ml of 30% HNO<sub>3</sub> was steadily added in to the mixture to keep the PH level. After that solution was stirred at stable temperature of 60 °C for 4 hours waiting to gel formation. Then gel was dried at temperature of 80 °C for 10 hours in an oven. Finally the gel was annealed at 500 °C temperature for 2 hours to get powder form. Now TiO<sub>2</sub> NPs in crystal form are ready. For this synthesis of Ag doped TiO<sub>2</sub> NPs, the same procedure was followed, having only difference having addition of AgNO<sub>3</sub> into TiO<sub>2</sub> solution in varying concentration as of 5% to 20%

### **2.1. Cell culturing and cytotoxic activity of nano particles**

The cytotoxic activity of NPs was judged the human liver cancer cells (HepG2). The cells were cultured having standards condition of 37 °C, 95% humidity and 5% CO<sub>2</sub>. The HepG2 cells were plated on to 6-well plate of density  $6.0 \times 10^5$  cells per well and incubated for 24 hours at constant temperature of 37 °C. The efficiency and distribution of samples were evaluated by phase contrast microscopy. The HepG2 cells were exposed to the NPs suspension and were incubated at temperature of 37 °C for 24 hours, after that the cells were washed thrice with PBS (PH 7.4). The cells were then suspended in 2% FBS (v/v), balanced in cell plates, and examined by fluorescence intensity in FACSCalibur fluorescence-activated cell sorter (FACS™) with CellQuest to conclude the cell counts for every sample

## **3. Results and discussion**

### **3.1. XRD analysis**

The X-rays diffraction (XRD) technique was applied to examine the crystallographic structure of both un-doped and Ag-doped TiO<sub>2</sub> NPs. The XRD pattern of all the samples is presented in Figure 1. The patterns reveal that the nanoparticles exist in two phases: Brookite and Rutile. The Brookite phase has an orthorhombic structure, while the Rutile phase has a tetragonal structure. Phase identification was performed by comparing the patterns with reference data cards for TiO<sub>2</sub> (Rutile: pdf # 21-1276, Brookite: pdf # 29-1360). The XRD patterns of the Ag-doped TiO<sub>2</sub> samples closely resemble those of pure TiO<sub>2</sub>, with no diffraction peaks corresponding to

silver, indicating that the metal particles are evenly dispersed within the TiO<sub>2</sub> matrix. The doping of Ag did not alter the TiO<sub>2</sub> crystal structure, suggesting that the silver ions replaced titanium in the crystal lattice. Therefore, no diffraction peaks related to silver or any new phases were observed in the XRD patterns. The crystallite size of the synthesized nanoparticles was determined by the Scherer method [28].

$$T = K \lambda / \beta \cos \theta$$

T= grain size

K= dimensionless shape factor

$\lambda$ = X-rays wavelength

$\beta$ = FWHM (in radians)

$\theta$ = Bragg's angle

The results are presented in table 1. The average crystallite size is around 15nm for all samples, calculated by Scherer formula.

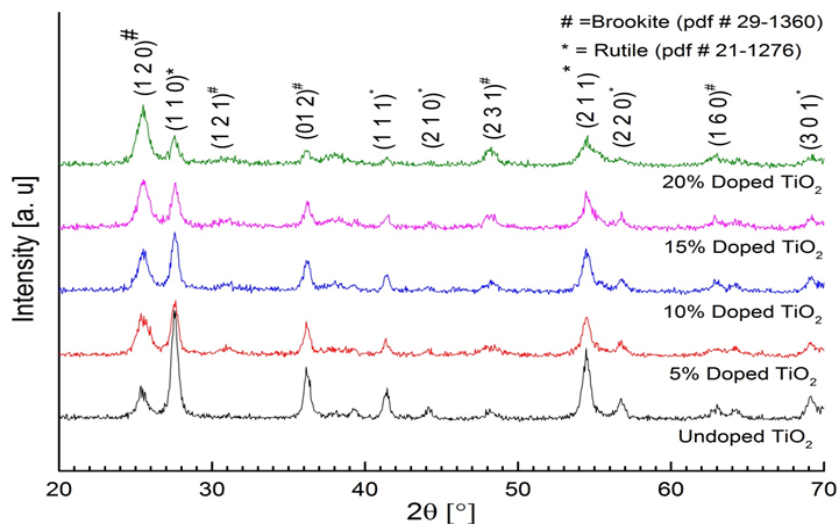


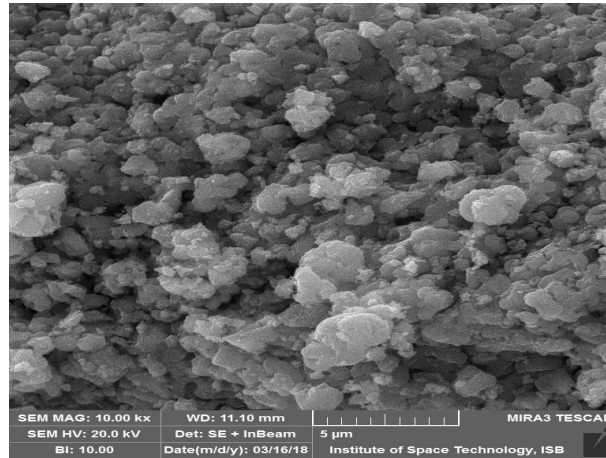
Fig.1. XRD Pattern for un doped TiO<sub>2</sub> and Ag-doped.

Table 1. FWHM and Crystallite size of bare TiO<sub>2</sub> and Ag-doped TiO<sub>2</sub>.

Sr. No	Sample	FWHM	CRYSTALLITE SIZE(nm)
1	Un-doped TiO <sub>2</sub>	0.544	15.709
2	5% doped TiO <sub>2</sub>	0.554	15.430
3	10% doped TiO <sub>2</sub>	0.543	15.140
4	15% doped TiO <sub>2</sub>	0.576	14.840
5	20% doped TiO <sub>2</sub>	0.580	14.740

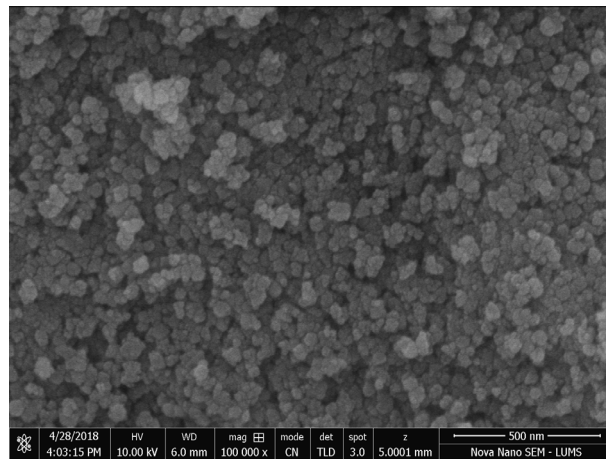
### 3.2. SEM analysis

To examine the surface morphology of the synthesized un-doped TiO<sub>2</sub> and Ag-doped TiO<sub>2</sub> nanoparticles, SEM analysis was performed. Figure 2 displays the SEM image of the un-doped TiO<sub>2</sub> nanoparticles. This image, taken at a magnification of 100,000x, shows aggregates made up of smaller particles with diameters ranging from 15 nm to 20 nm.



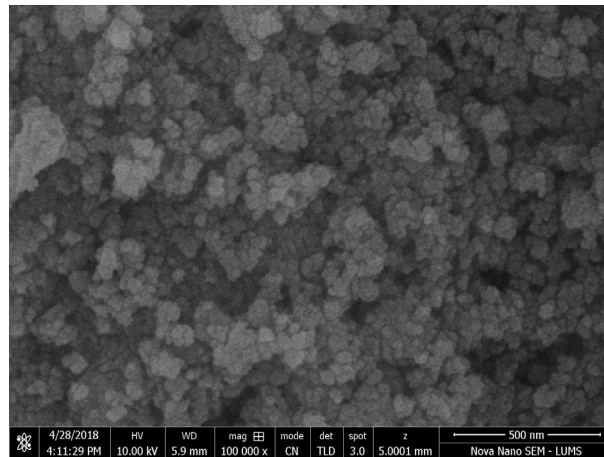
*Fig.2. SEM IMAGE OF UNDOPED TiO<sub>2</sub>.*

Figure 3 presents the SEM image of 5% Ag-doped TiO<sub>2</sub> nanoparticles. This image, magnified at 100,000x, shows that the average nanoparticle size is 14.63 nm, with a diameter array starting 11.46 nm to 19.11 nm. Findings indicate that Ag doping has reduced the size of the TiO<sub>2</sub> nanoparticles. This size reduction is attributed to the dopant ions trapping the grain boundaries of the host material, which restricts grain growth and thus decreases the particle size [29]. Similar results have been observed in other studies [29,30,31].



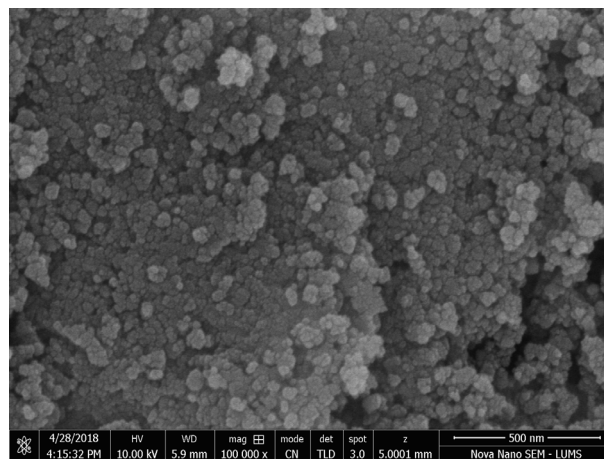
*Fig.3. SEM Image of 5% doped TiO<sub>2</sub>.*

Figure 4 shows the SEM image of 10 % Ag-doped TiO<sub>2</sub> nanoparticles. This image (magnified 100000x) reveals that the nanoparticles average size is 14.66nm and range of diameter is 11.60 nm to 19.50nm



*Fig.4. SEM Image of 10% doped TiO<sub>2</sub>.*

Figure 5 shows the SEM image of 15 % Ag-doped TiO<sub>2</sub> nanoparticles. This image (magnified 100000x) reveals that the nanoparticles average size is 14.48nm and range of diameter is 11.71nm to 19.81nm.



*Fig.5. SEM Image of 15% doped TiO<sub>2</sub>.*

Figure 6 shows the SEM image of 5 % Ag-doped TiO<sub>2</sub> nanoparticles. This image (magnified 100000x) reveals that the nanoparticles average size is 16.64nm and range of diameter is 10.88nm to 24.32nm.

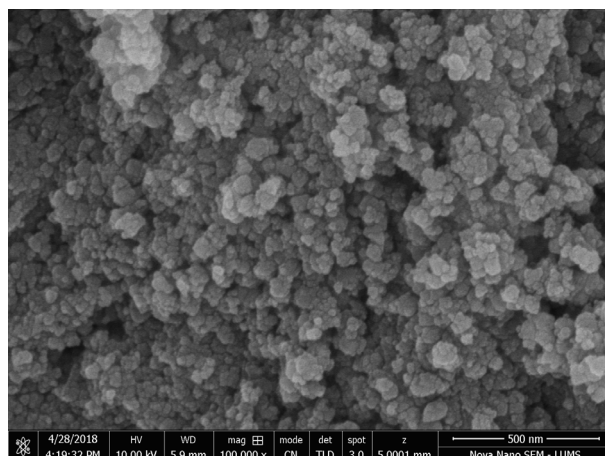


Fig.6. SEM Image of 20% doped  $\text{TiO}_2$ .

### 3.3. EDX analysis

EDX analysis was conducted to verify the doping and determine the atomic percentage of the dopant. In Figure 7, the EDX analysis shows no doping, while Figs. 8-11 confirm the presence of doping with atomic percentages of 0.367 at%, 0.706 at%, 0.834 at%, and 1.005 at%, respectively. Tables 2-6 display the weight and atomic percentages of all elements present in the sample. These results confirm the percentage doping if silver in  $\text{TiO}_2$  NPs.

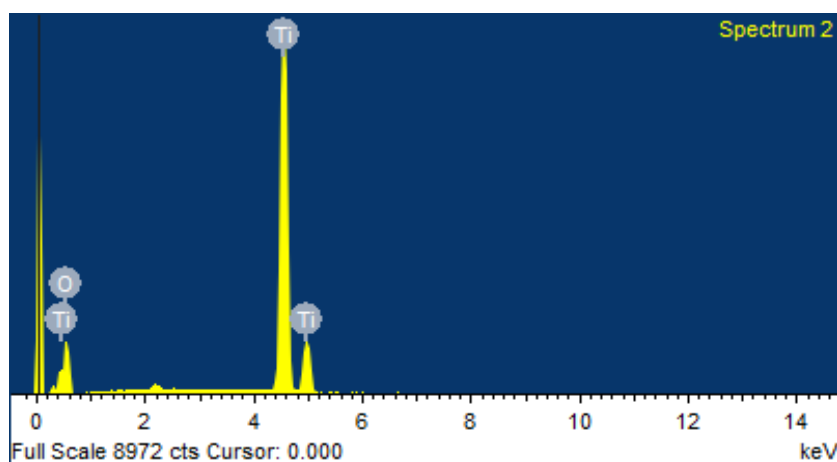


Fig. 7. EDX Spectrum of 0% doped  $\text{TiO}_2$ .

Table 2. Weight % and Atomic % of un-doped  $\text{TiO}_2$ .

Element	Weight %	Atomic %
O	38.67	65.37
Ti	61.33	34.63
<b>Total</b>	<b>100%</b>	<b>100%</b>

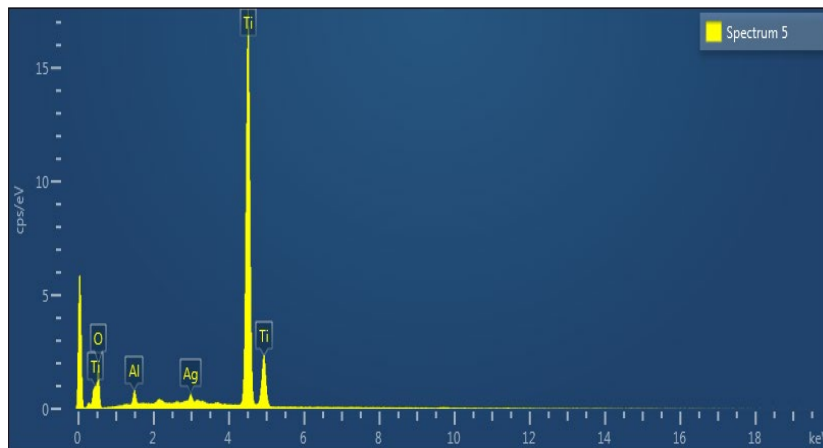


Fig.8. EDX Spectrum of 0.367 at% silver doped  $\text{TiO}_2$ .

Table 3. Weight % and Atomic % of 5 Percent Doped  $\text{TiO}_2$ .

Element	Weight %	Atomic %
O	44.72	70.656
Ti	52.15	27.524
Ag	1.57	0.367
Al	1.55	1.451
<b>Total</b>	<b>100%</b>	<b>100%</b>

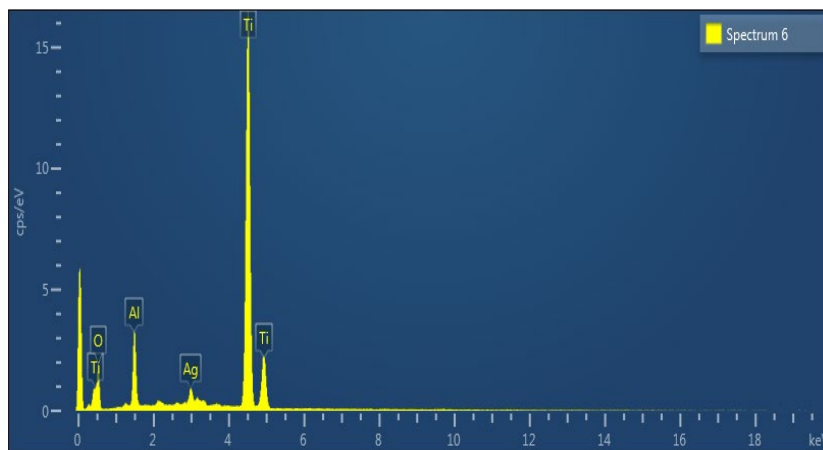


Fig.9.EDX Spectrum of 0.706 at% silver doped  $\text{TiO}_2$ .

Table 4. Weight % and Atomic % of 10 Percent Doped  $\text{TiO}_2$ .

Element	Weight %	Atomic %
O	41.47	66.525
Ti	48.34	25.904
Ag	2.97	0.706
Al	7.22	6.863
<b>Total</b>	<b>100%</b>	<b>100%</b>

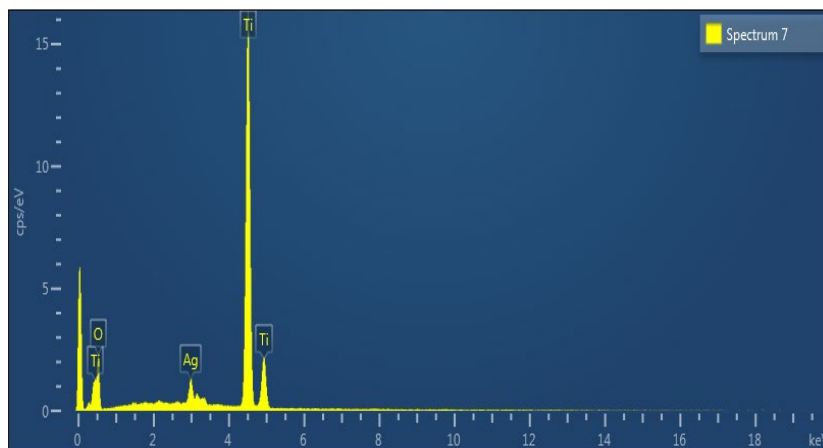


Fig.10. EDX Spectrum of 0.834 at % silver doped  $\text{TiO}_2$ .

Table 5. Weight % and Atomic % of 15 Percent Doped  $\text{TiO}_2$ .

Element	Weight %	Atomic %
O	45.15	71.830
Ti	51.15	27.183
Ag	3.54	0.834
Al	0.16	0.150
<b>Total</b>	<b>100%</b>	<b>100%</b>

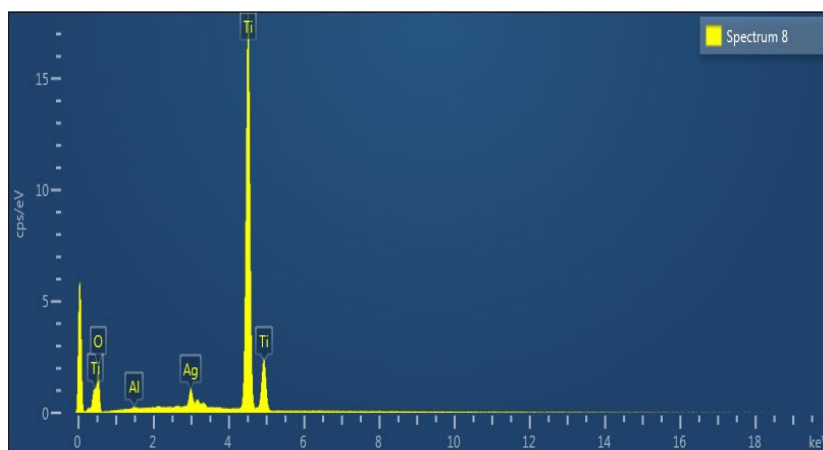


Fig.11. EDX Spectrum of 1.005 at% silver doped  $\text{TiO}_2$ .

Table 6. Weight % and Atomic % of 20 Percent Doped  $\text{TiO}_2$ .

Element	Weight %	Atomic %
O	48.06	74.400
Ti	47.56	24.594
Ag	4.38	1.005
<b>Total</b>	<b>100%</b>	<b>100%</b>

### 3.4. UV-Vis spectroscopy study

UV-Vis spectroscopy is used to examine the optical property of samples. The UV-Vis absorption spectrum of un-doped TiO<sub>2</sub> and Ag-doped TiO<sub>2</sub>, as shown in Figure 12, reveal a distinct band edge in the UV range of 400–450 nm, which is connected with the photo-excitation from the valence band to the conduction band. Figure 12 illustrates the absorption profiles of both un-doped TiO<sub>2</sub> and Ag-TiO<sub>2</sub> composites by varying silver content. These profiles demonstrate typical absorption characteristics, with a shift in the absorption spectra in the 400-450 nm range in the visible region, ascribed to the surface Plasmon resonance of silver. This shift in the absorption spectra suggests an interaction between Ag and Ti, which is consistent with the XRD patterns. The band gap is determined by plotting photonic power ( $E=h\nu$ ) on the X-axis plus  $(\alpha h\nu)^2$  on the Y-axis, using the Tauc equation [32] and plotted in figure 13

$$\alpha h\nu = A(h\nu - E_g)^m$$

Anywhere  $\alpha$  is absorption coefficient. ( $h\nu$ ) is the photonic energy, for direct optical transition  $m= 1/2$ ,  $E_g$  is the optical band gap and  $A$  is a constant. Table 7 shows the values of band gaps related to un-doped TiO<sub>2</sub> NPs and Ag-doped TiO<sub>2</sub> NPs the results shows that the band gap of TiO<sub>2</sub> decreases with increasing doping quantity of silver which enhanced the optical properties. Figure 13 shows the graphs of band gap.

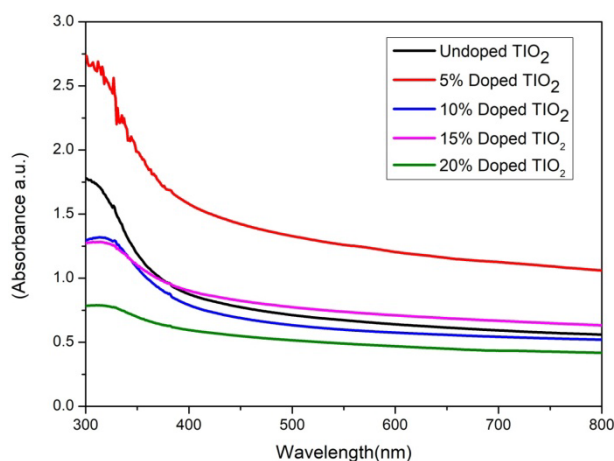


Fig.12. Uv-Vis spectra of un-doped and Ag-doped TiO<sub>2</sub> nanoparticles.

Table 7. Band Gaps of un-doped and Ag- Doped TiO<sub>2</sub>.

Sr No	Name	Band Gap
1	Undoped TiO <sub>2</sub>	3.31
2	5% Doped TiO <sub>2</sub>	3.15
3	10% doped TiO <sub>2</sub>	3.11
4	15% doped TiO <sub>2</sub>	2.96
5	20% doped TiO <sub>2</sub>	2.91

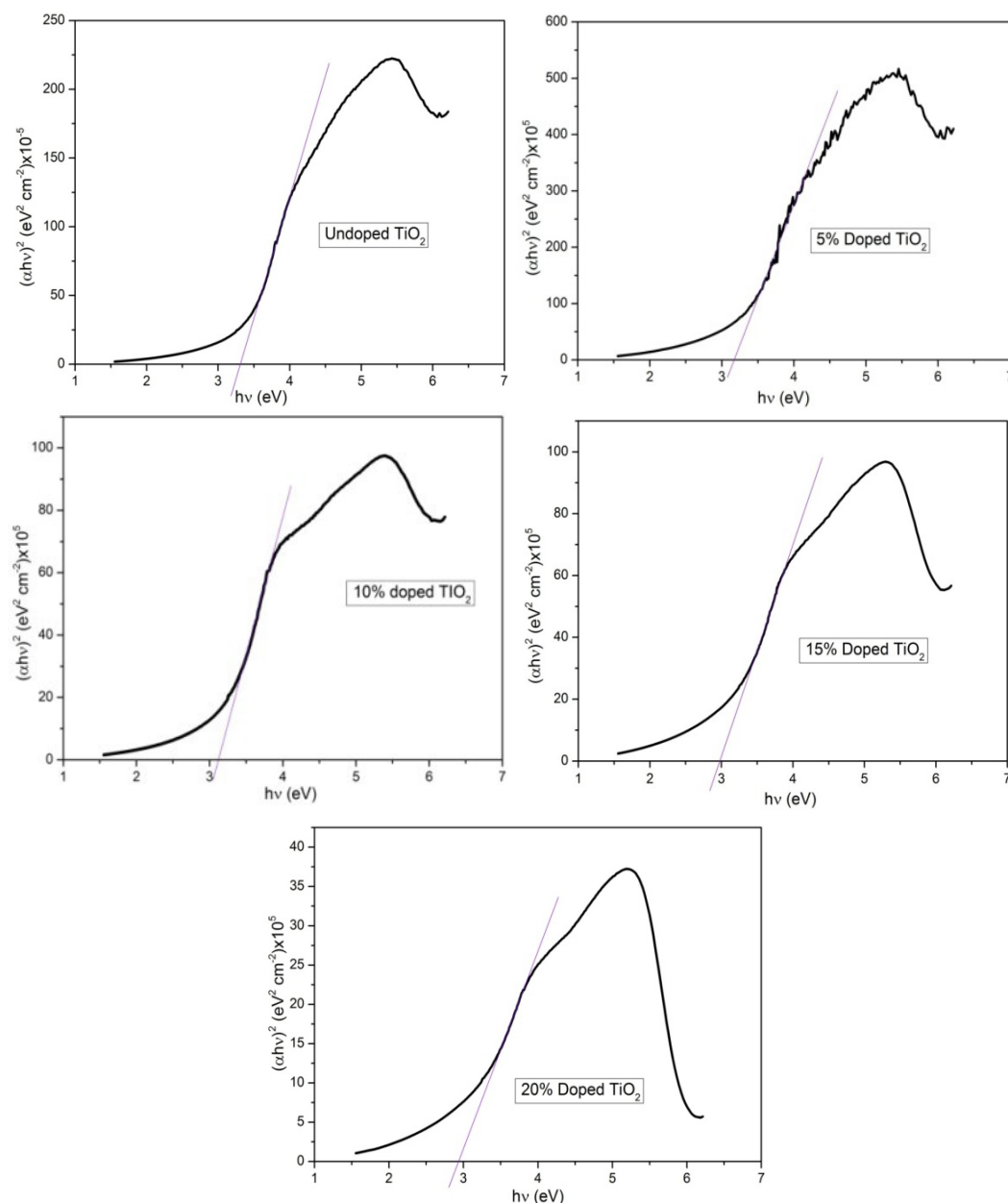


Fig. 13. Band gap of un-doped  $\text{TiO}_2$  and doped with 5%, 10%, 15% and 20%.

#### 4. Cytotoxicity analysis

Ag-doped  $\text{TiO}_2$  nanoparticles with varying concentrations (5%, 10%, 15%, and 20%) were exposed to human liver cancer cells (HepG2) for 24 hours, with cell viability be assessed with the MTT assay, a tool for measuring cell proliferation inhibition [32,33]. The findings showed that Ag-doped NPs decreased cell viability in a concentration-dependent approach. As the concentration of ag-doping in  $\text{TiO}_2$  NPs increased, the cell viability was decreased. The cytotoxic approach of NPs could be credited by following factors:

- (1) The cytotoxic effect of NPs may result from oxidative stress, caused by ROS generation or a reduction in antioxidants [34, 35, 36].
- (2) Reactive oxygen species, such as hydroxyl radicals ( $\text{HO}\cdot$ ), superoxide anions ( $\text{O}_2^-$ ), and hydrogen peroxide ( $\text{H}_2\text{O}_2$ ), have various physiological and cellular impacts, including DNA damage and apoptosis [36,37]. Our result indicated to ROS generation by the nanoparticles was

directly proportional towards Ag doping concentration in TiO<sub>2</sub> nanoparticles which decrease the cell viability, as shown in Figure 14.

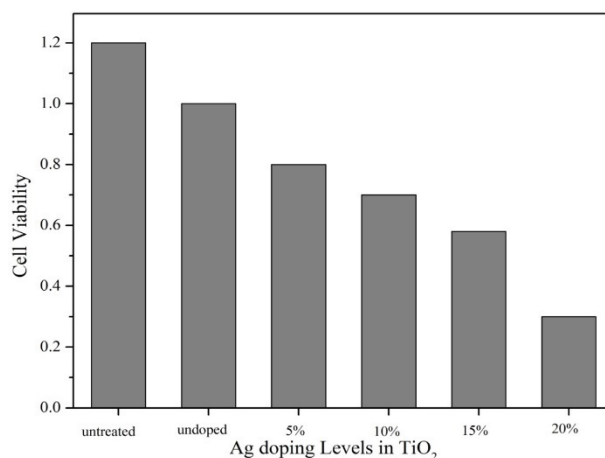


*Fig. 14. Cytotoxic effects of doped and un-doped samples.*

It has been observed that the ROS generation in nanoparticles can effectively target and kill cancerous cells while having minimal impact on normal cells [38, 39]. These findings indicate that Ag-doped TiO<sub>2</sub> nanoparticles exhibit anticancer properties, with metal-based nanoparticles being investigated as potential agents for killing cancer cells [40, 41, 42, 43]. Additionally, the anticancer activity enhances as the Ag doping percentage in TiO<sub>2</sub> nanoparticles increases

## 5. Conclusion

The Ag-doped TiO<sub>2</sub> NPs were synthesized and successfully characterized by SEM, XRD, EDX and UV-Vis spectra. XRD pattern appearances the Brookite and rutile phase which remains same upon doing with Ag. The average calculated crystalline size of sample is 15 nm. The SEM images show that the doing of Ag influences the size of TiO<sub>2</sub> NPs which reduces its size. The EDX spectroscopy confirmed the doping of Ag in TiO<sub>2</sub>. The UV-Vis absorption spectra showed that the band gap decreases by increasing the silver doping which reflects the enhanced absorption of light and also improve optical properties. The cytotoxic behavior was determined by MTT assay, tested on human liver cancer cells. The results concluded that increase in Ag-doping directed to reduction of cell viability. These findings suggested that Ag-doped TiO<sub>2</sub> NPs have potential of anticancer activity which is proportional to Ag doping

## Funding

Researchers supporting project number (RSPD2025R952), King Saud University.

## Acknowledgement

The authors would like to thank the Researchers Supporting Project number (RSPD2025R952), King Saud University, Riyadh, Saudi Arabia.

## References

- [1] Choi, H., Stathatos, E., Dionysiou, D. D. (2006), *Applied Catalysis B: Environmental*, 63(1-2), 60-67; <https://doi.org/10.1016/j.apcatb.2005.09.012>
- [2] de Jesus, R. A., Oliveira, Í. M., Nascimento, V. R. S., Ferreira, L. F. R., Figueiredo, R. T. (2023), *Novel Platforms for Drug Delivery Applications* (pp. 437-457), Woodhead Publishing; <https://doi.org/10.1016/B978-0-323-91376-8.00018-5>
- [3] Fadeel, D. A. A., Hanafy, M. S., Kelany, N. A., Elywa, M. A. (2021), *Heliyon*7(6); <https://doi.org/10.1016/j.heliyon.2021.e07370>
- [4] Cazan, C., Enesca, A., Andronic, L. (2021), *Polymers* 13(12), 2017; <https://doi.org/10.3390/polym13122017>
- [5] Bayat, N., Lopes, V. R., Schölermann, J., Jensen, L. D., Cristobal, S. (2015), *Biomaterials* 63, 1-13; <https://doi.org/10.1016/j.biomaterials.2015.05.044>
- [6] Jiang, T., Hou, L., Rahman, S. M., Gong, Z., Bai, X., Vulpe, C., Gu, A. Z. (2024), *Journal of Hazardous Materials* 134850; <https://doi.org/10.1016/j.jhazmat.2024.134850>
- [7] Inoue, S., Matsuo, I., Matsumura, Y. (2024), *Ionics*, 30(9), 5473-5479; <https://doi.org/10.1007/s11581-024-05674-3>
- [8] Ramacharyulu, P. V. R. K., Prasad, G. K., Srivastava, A. R. (2015), *RSC Advances*, 5(2), 1309-1314; <https://doi.org/10.1039/C4RA10249E>
- [9] Assis, M. D., Gouveia, A. F., Ribeiro, L. K., Ponce, M. A., Churio, M. S., Oliveira Jr, O. N., Andres, J. (2023), *Applied Catalysis A: General*, 652, 119038; <https://doi.org/10.1016/j.apcata.2023.119038>
- [10] Radivoievych, A., Prylutska, S., Zolk, O., Ritter, U., Frohme, M., Grebinyk, A. (2023), *Pharmaceutics*, 15(11), 2616; <https://doi.org/10.3390/pharmaceutics15112616>
- [11] Yuan, M., Zhong, S., Li, G., Fan, G., Yu, X. (2024), *Fuel*, 358, 130200; <https://doi.org/10.1016/j.fuel.2023.130200>
- [12] Gatou, Maria-Anna, Athanasia Syrrakou, Nefeli Lagopati, Evangelia A. Pavlatou. *Reactions* 5, no. 1 (2024): 135-194; <https://doi.org/10.3390/reactions5010007>
- [13] Rosário, F., Bessa, M. J., Brandão, F., Costa, C., Lopes, C. B., Estrada, A. C., Reis, A. T. (2020), *Nanomaterials*, 10(3), 447; <https://doi.org/10.3390/nano10030447>
- [14]. Aravind, M., Amalanathan, M., Aslam, S., Noor, A. E., Jini, D., Majeed, S., Sillanpaa, M. (2023), *Chemosphere*, 321, 138077; <https://doi.org/10.1016/j.chemosphere.2023.138077>
- [15]. Uyen, N. N., Tuyen, L. T. C., Hieu, L. T., Nguyen, T. T. T., Thao, H. P., Do, T. C. M. V., Luo, C. W. (2022), *Coatings*, 12(12), 1957; <https://doi.org/10.3390/coatings12121957>
- [16] Hao, C., Wang, Y., Hu, S., Guo, X. (2023), *Applied Catalysis A: General*, 663, 119326; <https://doi.org/10.1016/j.apcata.2023.119326>
- [17]. Feng, N., Lin, H., Song, H., Yang, L., Tang, D., Deng, F., Ye, J. (2021), *Nature Communications*, 12(1), 4652; <https://doi.org/10.1038/s41467-021-24912-0>
- [18] Wang, Y., Wang, C., Luo, P., & Hu, Q. (2023), *Applied Surface Science*, 614, 156251; <https://doi.org/10.1016/j.apsusc.2022.156251>
- [19]. Ji, L., Qin, X., Zheng, J., Zhou, S., Xu, T., Shi, G. (2020), *Journal of Sol-Gel Science and Technology*, 93, 291-301; <https://doi.org/10.1007/s10971-019-05197-8>
- [20] Lin, B. L., Chen, R., Zhu, M. L., She, A. S., Chen, W., Niu, B. T., Lin, X. M. (2024), *Catalysts*, 14(9), 639; <https://doi.org/10.3390/catal14090639>
- [21] Bai, C., Zhao, J., Su, J., Chen, J., Cui, X., Sun, M., Zhang, X. (2022), *Life Sciences*, 306, 120804; <https://doi.org/10.1016/j.lfs.2022.120804>
- [22]. Lee, S. Y., Kim, I. Y., Heo, M. B., Moon, J. H., Son, J. G., Lee, T. G. (2021), *Biomolecules*, 11(3), 375; <https://doi.org/10.3390/biom11030375>
- [23] Almutairi, B., Ali, D., Alyami, N., Alothman, N. S., Alakhtani, S., Alarifi, S. (2021), *Journal*

- of King Saud University-Science, 33(6), 101546; <https://doi.org/10.1016/j.jksus.2021.101546>
- [24]Mahjoubian, M., Sadat Naeemi, A., Sheykhan, M. (2024), Biological Trace Element Research, 1-19; <https://doi.org/10.1007/s12011-024-04127-2>
- [25]. Munir, T., Mahmood, A., Abbas, N., Sohail, A., Khan, Y., Rasheed, S., Ali, I. (2024), ACS omega, 9(32), 34841-34847; <https://doi.org/10.1021/acsomega.4c04183>
- [26]Batool, A., Azizullah, A., Ullah, K., Shad, S., Khan, F. U., Seleiman, M. F., Zeb, U. (2024), BMC Plant Biology, 24(1), 820; <https://doi.org/10.1186/s12870-024-05525-3>
- [27] Shabaninia, M., Khorasani, M., Baniyaghoob, S. (2024), ChemistrySelect, 9(14), e202303358; <https://doi.org/10.1002/slct.202303358>
- [28] Khalid, A. D., Hadi, F., Iqbal, S. S., Buzdar, S. A., Khan, A. K. (2022), Digest Journal of Nanomaterials & Biostructures, 17(1); <https://doi.org/10.15251/DJNB.2022.171.73>
- [29]Khan, M. M., Kumar, S., Khan, M. N., Ahamed, M., Al Dwayyan, A. S. (2014). Journal of luminescence, 155, 275-281; <https://doi.org/10.1016/j.jlumin.2014.06.007>
- [30]Munir, T., Mahmood, A., Abbas, N., Sohail, A., Khan, Y., Rasheed, S., Ali, I. (2024), ACS omega, 9(32), 34841-34847; <https://doi.org/10.1021/acsomega.4c04183>
- [31] Ahamed, M., Khan, M. M., Akhtar, M. J., Alhadlaq, H. A., Alshamsan, A. (2017), Scientific reports, 7(1), 17662; <https://doi.org/10.1038/s41598-017-17559-9>
- [32] Alsaleh, N. B., Aljarbou, A. M., Assal, M. E., Assiri, M. A., Almutairi, M. M., As Sobeai, H. M., Adil, S. F. (2024), Pharmaceuticals, 17(2), 168; <https://doi.org/10.3390/ph17020168>
- [33]González-Ballesteros, N., Diego-González, L., Lastra-Valdor, M., Grimaldi, M., Cavazza, A., Bigi, F., Simón-Vázquez, R. (2021), Materials Science and Engineering: C, 123, 111960; <https://doi.org/10.1016/j.msec.2021.111960>
- [34]. Ahamed, M., Akhtar, M. J., Alhadlaq, H. A. (2023), Journal of King Saud University-Science, 35(6), 102750; <https://doi.org/10.1016/j.jksus.2023.102750>
- [35]Park, S., Eom, T. Y., Jeong, R. H., Lee, H. J., Boo, J. H. (2024), Applied Surface Science, 657, 159746; <https://doi.org/10.1016/j.apsusc.2024.159746>
- [36]Wang, Y., Liang, X., He, F., Tang, H., Yin, X., Andrikopoulos, N., Ke, P. C. (2023, November), Proceedings (Vol. 92, No. 1, p. 5). MDPI; <https://doi.org/10.3390/proceedings2023092005>
- [37] Lin, G. S. S., Lestari, W., Muhamad Halil, M. H., Abd Aziz, M. S. (2024), Odontology, 1-9; <https://doi.org/10.1007/s10266-024-01012-1>
- [38] Chatterjee, S., Sil, P. C. (2024), Chemical Research in Toxicology, 37(10), 1612-1633; <https://doi.org/10.1021/acs.chemrestox.4c00235>
- [39] Cao, J., Wu, Q., Liu, X., Zhu, X., Huang, C., Wang, X., Song, Y. (2024), Journal of Environmental Sciences; <https://doi.org/10.1016/j.jes.2024.03.009>
- [40]Makvandi, P., Wang, C. Y., Zare, E. N., Borzacchiello, A., Niu, L. N., Tay, F. R. (2020), Advanced Functional Materials, 30(22), 1910021; <https://doi.org/10.1002/adfm.201910021>
- [41] Khalid, A. D., Iqbal, S. S., Buzdar, S. A., Ahmad, M. (2021), Journal of Nanoscope (JN), 2(2), 185-197; <https://doi.org/10.52700/jn.v2i2.34>
- [42]Ibáñez-Moragues, M., Fernández-Barahona, I., Santacruz, R., Oteo, M., Luján-Rodríguez, V. M., Muñoz-Hernando, M., Morcillo, M. Á. (2023), Molecules, 28(19), 6874; <https://doi.org/10.3390/molecules28196874>
- [43]Cem, Ö. Z. İ. Ç., Yildiz, B., Demirel, R., & Özden, Ö. (2024), Kafkas Üniversitesi Veteriner Fakültesi Dergisi, 30(4).